ISSN 0023-1584, Kinetics and Catalysis, 2007, Vol. 48, No. 4, pp. 490–504. © MAIK "Nauka/Interperiodica" (Russia), 2007.
Original Russian Text © E.P. Talsi, K.P. Bryliakov, N.V. Semikolenova, V.A. Zakharov, M. Bochmann, 2007, published in Kinetika i Kataliz, 2007, Vol. 48, No. 4, pp. 521–536.

MECHANISMS OF CATALYTIC REACTIONS

Key Intermediates in Metallocene- and Post-metallocene-Catalyzed Polymerization

E. P. Talsi[a], K. P. Bryliakov[a], N. V. Semikolenova[a], V. A. Zakharov[a], and M. Bochmann[b]

[a] *Boreskov Institute of Catalysis, Siberian Branch, Russian Academy of Sciences, Novosibirsk, 630090 Russia*

[b] *University of East Anglia, Norwich, NR4 7TJ, UK*

e-mail: talsi@catalysis.nsk.su

Received June 23, 2006

Abstract—The structures of intermediates formed upon the activation by methylaluminoxane (MAO) of a wide range of metallocene and post-metallocene catalysts of olefin polymerization were studied by ^{13}C, ^{1}H, and ^{19}F NMR. For all metallocenes considered (L_2ZrCl_2 and L_2TiCl_2), under conditions similar to real polymerization conditions (Al/Zr > 200), two types of intermediates were identified in the reaction solution, namely, heterodinuclear ion pairs $[L_2\mathbf{M}(\mu\text{-Me})_2AlMe_2]^+[Me\text{–}MAO]^-$ (**III**) and zwitterionic intermediates $L_2\mathbf{M}Me^+\text{◄—}Me\text{–}Al^-\equiv MAO$ (**IV**) (**M** = Zr, Ti). The relative concentration of **III** increases with an increase in the Al/Zr ratio. In the post-metallocene/MAO catalytic systems, the reaction solution can be dominated either by heterodinuclear pairs of type **III** (bis(imino)pyridyl iron complexes) or by zwitterionic intermediates of type **IV** (half-titanocenes, complexes with restricted geometry). Both species **III** and species **IV** catalyze olefin polymerization. Both the species initiating polymerization, $[L'_2TiMe(S)]^+[Me\text{–}MAO]^-$, and the species responsible for chain growth, $[L\ [L'_2TiP]^+[Me\text{–}MAO]^-$ (P is the polymer chain, and S is a solvent molecule), were characterized in the bis(phenoxyimine) titanium complex/MAO system.

DOI: 10.1134/S0023158407040052

Approximately 100 million tons of polyethylene and polypropylene are produced annually in the world. Most of these polymers are obtained by catalytic polymerization. It is, therefore, clear why both academic and applied sciences show rapt interest in new polymerization catalysts, which could improve the efficiency of the presently existing processes and afford new polymers. The metallocene complexes of Zr and Hf and so-called post-metallocene complexes, such as the zirconium and titanium phenoxyimine complexes and iron bis(imino)pyridyl complexes [1–7], have attracted the greatest attention in recent years.

New catalysts are often discovered by a fluke. For more rational search for polymerization catalysts, one should know the main factors determining their activity, selectivity, and stability. As a rule, polymerization catalysts include at least two components, namely, a transition metal complex and an activating compound. The role of the activator is the methylation of the initial chloride complex and the abstraction of the Me anion from the metal to form an ion pair in which the cation contains either a weakly coordinated counterion or a solvent molecule in the vacant coordination site. Such Lewis acids as methylaluminoxane (MAO), $B(C_6F_5)_3$, or $[CPh_3]^+[B(C_6F_5)_4]^-$ can be used as activators. In the present report, we summarize the results of our studies mainly aimed at revealing how metallocenes and post-metallocenes are activated and deactivated under the action of the most frequently used activator MAO [8–14].

Structures of the Intermediates Resulting from the Activation of Metallocenes by MAO

Cp_2ZrMe_2(Cp_2ZrCl_2)/MAO. MAO remains the activator most frequently used for metallocene and post-metallocene polymerization catalysts. It is a poorly characterized mixture of oligomeric products of $AlMe_3$ hydrolysis. For this reason, attempts to determine the structure of complexes resulting from the interaction of metallocenes with MAO were long considered as having no prospects. However, ^{1}H and ^{13}C NMR studies performed in the last decade have demonstrated that the structure of the cationic moiety of the ion pairs formed during the interaction of the metallocenes with MAO can be determined rather reliably [7–14]. The structure of the Zr-I–Zr-IV intermediates formed in the Cp_2ZrMe_2/MAO system [8] is shown in Fig. 1. The assignment of the NMR signals of Zr-I–Zr-IV is based on the detailed spectroscopic data obtained for the cationic complexes $L_2Zr(CH_3)^+\cdots H_3CB(C_6F_5)_3^-$, $[(L_2ZrMe)_2(\mu\text{-Me})]^+[B(C_6F_5)_4]^-$, $[L_2ZrMe^+\cdots B(C_6F_5)_4^-]$, and $[L_2Zr(\mu\text{-Me})_2AlMe_2]^+[B(C_6F_5)_4]^-$ [15–20]. The key problem in the determination of the structure of the

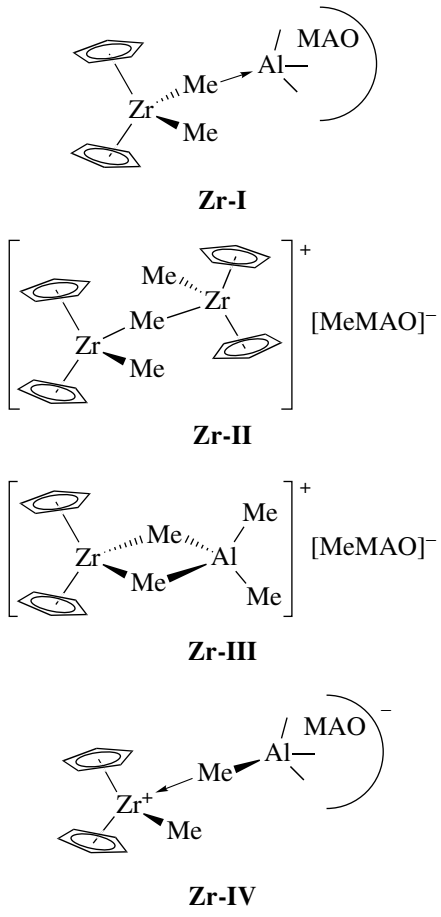

Fig. 1. Assumed structures of the Zr-I–Zr-IV intermediates resulting from the interaction of Cp_2ZrMe_2 with MAO [8].

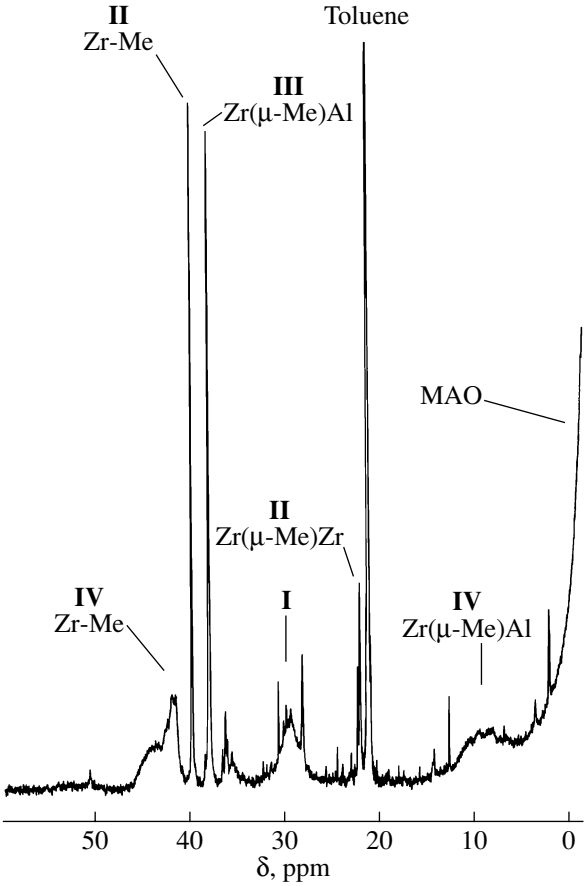

Fig. 2. ^{13}C NMR spectra of the Cp_2ZrMe_2/MAO* system in the region of methyl groups (MAO* is MAO enriched in the ^{13}C isotope); $[Al]_\Sigma = 1.8$ mol/l, Al/Zr = 100, toluene, T = –25°C [8].

Zr-IV zwitterionic intermediate is to detect the ^{13}C NMR signals of the terminal (42 ppm) and bridging (9 ppm) methyl groups (Fig. 2). The chemical shifts for the structurally similar complex $Cp_2ZrMe(\mu\text{-}Me)Al(C_6F_5)_3$ (40.5 ppm for the terminal methyl group and 7.9 ppm for the bridging methyl groups) are similar to those for Zr-IV [21]. The intermediate Zr-I is a weak complex between Cp_2ZrMe_2 and MAO. The Zr-I and Zr-II complexes are observed only at small Al/Zr ratios (<100), whereas the Zr-III and Zr-IV complexes dominate in the solution at large Al/Zr ratios. In the Zr-II and Zr-III complexes, the oligomeric anion [Me-MAO]$^-$ is in the outer coordination sphere of zirconium and, hence, the nonuniformity of the [Me-MAO]$^-$ oligomers exerts a weak effect on the width of the NMR signals from the cationic moieties of Zr-II and Zr-III, which exhibit narrow NMR signals. By contrast, the intermediate Zr-IV exhibits broad signals due to the direct coordination of [Me-MAO]$^-$ to zirconium (Fig. 2).

Cp_2TiMe_2(Cp_2TiCl_2)/MAO. It is natural to expect that the ion pairs formed in the Cp_2TiCl_2/MAO and Cp_2ZrCl_2/MAO catalytic systems have similar structures. In complete accord with this assumption, the interaction of Cp_2TiCl_2 with MAO (Al/Ti = 5–300) afforded the following complexes: $Cp_2TiMeCl$, Cp_2TiMe_2, $[Cp_2TiMe(\mu\text{-}Cl)Cp_2TiCl]^+[Me\text{–}MAO]^-$ (**Ti-II$_1$**), $[Cp_2TiMe(\mu\text{-}Cl)Cp_2TiMe]^+[Me\text{–}MAO]^-$ (**Ti-II$_2$**), $[Cp_2TiMe(\mu\text{-}Me)Cp_2TiMe]^+[Me\text{–}MAO]^-$ (**Ti-II$_3$**), the heterodinuclear ion pair $[Cp_2Ti(\mu\text{-}Me)_2AlMe_2]^+[Me\text{–}MAO]^-$ (**Ti-III**), and the zwitterionic intermediate $Cp_2TiMe^+ \leftarrow\!\!-Me\text{–}Al^-\equiv MAO$ (**Ti-IV**) (Fig. 3) [11]. Under conditions close to real polymerization (Al/Ti = 100–300), the solution mainly contains the Ti-III and Ti-IV complexes (Fig. 4). The titanium complexes Ti-III and Ti-IV are much less stable than the corresponding zirconium complexes: the latter are stable for several weeks at room temperature, whereas the former decompose at this temperature within a few hours. The main pathway of the decomposition of the Ti^{4+} complexes is the reduction of Ti^{4+} to Ti^{3+} (see below).

It seems of interest to continue the study of the metallocene/MAO catalytic systems by considering com-

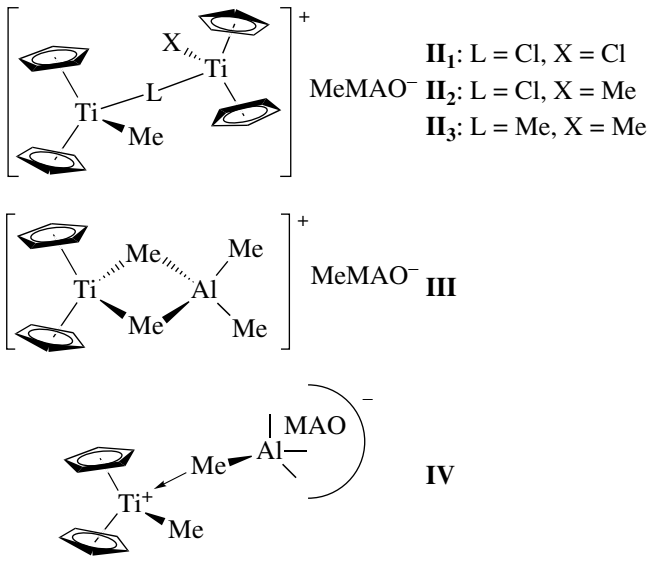

Fig. 3. Assumed structures of intermediates Ti-II–Ti-IV formed upon the interaction of Cp_2TiCl_2 with MAO [11].

plexes with substituted cyclopentadienyl and indenyl ligands, which are more promising for practice.

$(Cp–R)_2ZrCl_2$ (R = *n*-Bu)/MAO. The formation of the Zr-III and Zr-IV complexes and other zirconium species, which are present in the catalytic system at different Al/Zr ratios, was studied by recording the ^1H NMR spectra of the cyclopentadienyl ligands (Fig. 5). The signals of Zr-III were assigned by comparing the observed signals with the corresponding signals of the $[(Cp–n\text{-}Bu)_2Zr(\mu\text{-}Me)_2AlMe_2]^+[B(C_6F_5)_4]^-$ complex [9]. The ^1H NMR spectrum of the $(Cp–n\text{-}Bu)_2ZrCl_2$/MAO system in the region of cyclopentadienyl protons contains narrow signals of Zr-III and several broad signals designated as IV_1, IV_2, and IV_3, which can be assigned to different complexes of the Zr-IV type (Fig. 5, spectrum *1*). The observed spectrum simplifies as the Al/Zr ratio is increased. The complex Zr-III becomes the dominant species in the reaction solution (Fig. 5, spectra *2* and *3*). Catalytic data show that the $(Cp–n\text{-}Bu)_2ZrCl_2$/MAO system is inactive in ethylene polymerization at Al/Zr < 200. The catalytic activity at Al/Zr = 1000 is 13 times higher than that at Al/Zr = 200 (Table 1). According to NMR data, the fraction of Zr-III complexes in the reaction solution increases with an increase in Al/Zr. Under the polymerization conditions, the concentration of zirconium and MAO is 1–2 orders of magnitude lower than that in NMR experiments. Despite this, it is natural to expect that the fraction of Zr-III will increase with an increase in the Al/Zr ratio under the polymerization conditions as well. Thus, the observed increase in the catalytic activity of the $(Cp–n\text{-}Bu)_2ZrCl_2$/MAO system with an increase in the Al/Zr ratio can be attributed to the increase in the concentration of Zr-III dpecies. However, the Zr-III species exist only at the polymerization

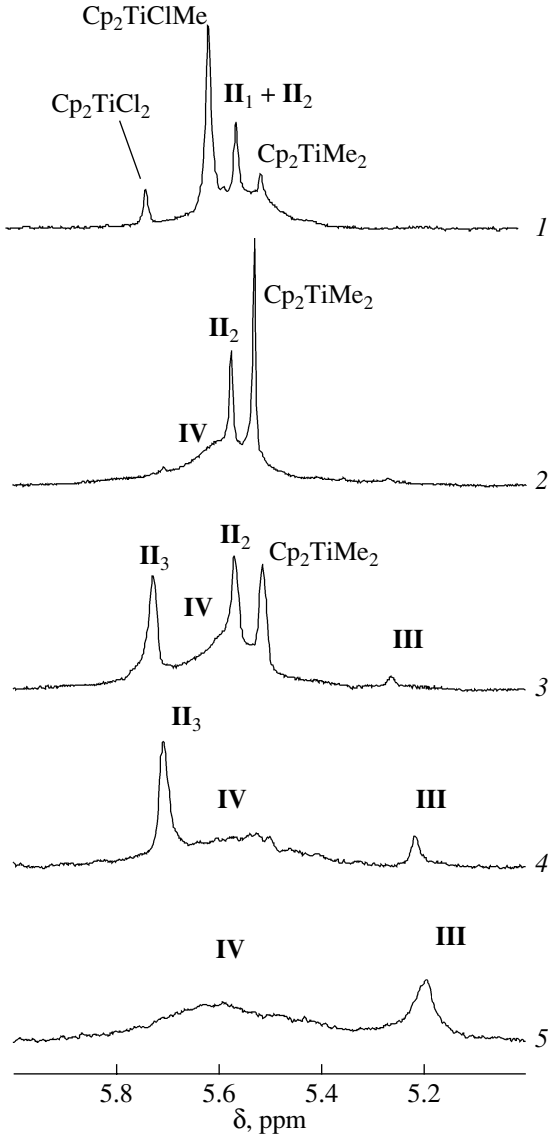

Fig. 4. ^1H NMR spectra of the Cp_2TiCl_2/MAO system in the region of hydrogen atoms of the Cp group at Al/Ti = (*1*) 10, (*2*) 20, (*3*) 40, (*4*) 90, and (*5*) 300; [Al] = 0.75 mol/l, toluene-d_8, T = –15°C [11].

initiation stage. Later, polymerization is continued by complexes in which one ligand is the growing polymer chain. Unfortunately, it is impossible to study this type of complex in this catalytic system. Evidently, an adjacent coordination site of zirconium should be occupied by a weakly coordinated molecule to efficiently continue polymerization by complexes containing the polymer chain as a ligand. At large Al/Zr ratios, only the strongest Lewis acid sites of MAO are involved in the abstraction of the Me anion from the zirconocene molecule. The $[Me–MAO]^-$ counterions resulting from this process can have a lowered coordinating power. Perhaps this fact also contributes to the increase in the activity of the catalyst with an increase in the Al/Zr

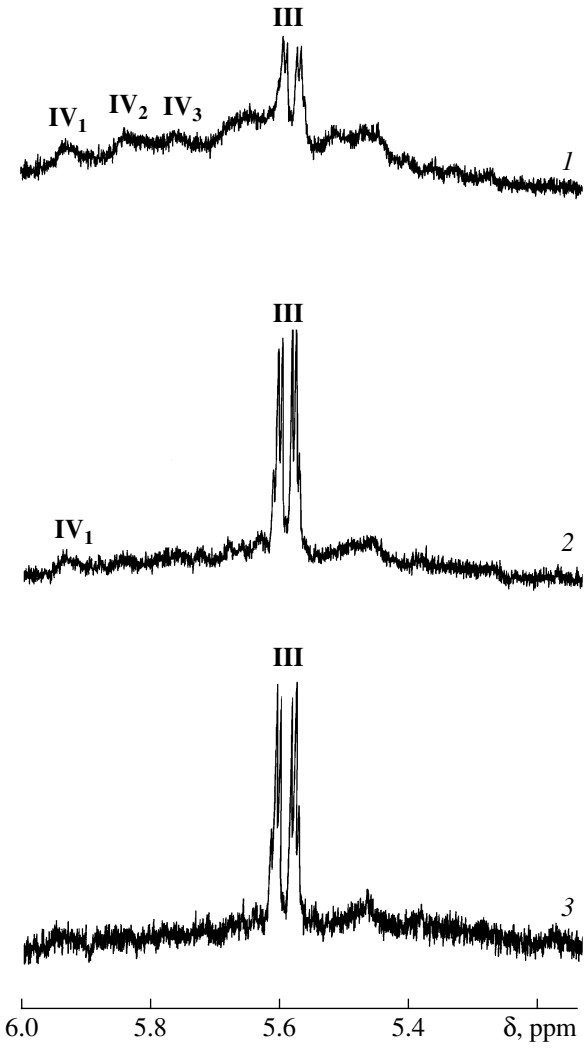

Fig. 5. ^{1}H NMR spectra of the (Cp–*n*-Bu)$_2$ZrCl$_2$/MAO system in the region of hydrogen atoms of the Cp group at Al/Zr = (*1*) 50, (*2*) 200, and (*3*) 600; [(Cp–*n*-Bu)$_2$ZrCl$_2$] = 10^{-3} mol/l, toluene-d$_8$, T = 20°C [9].

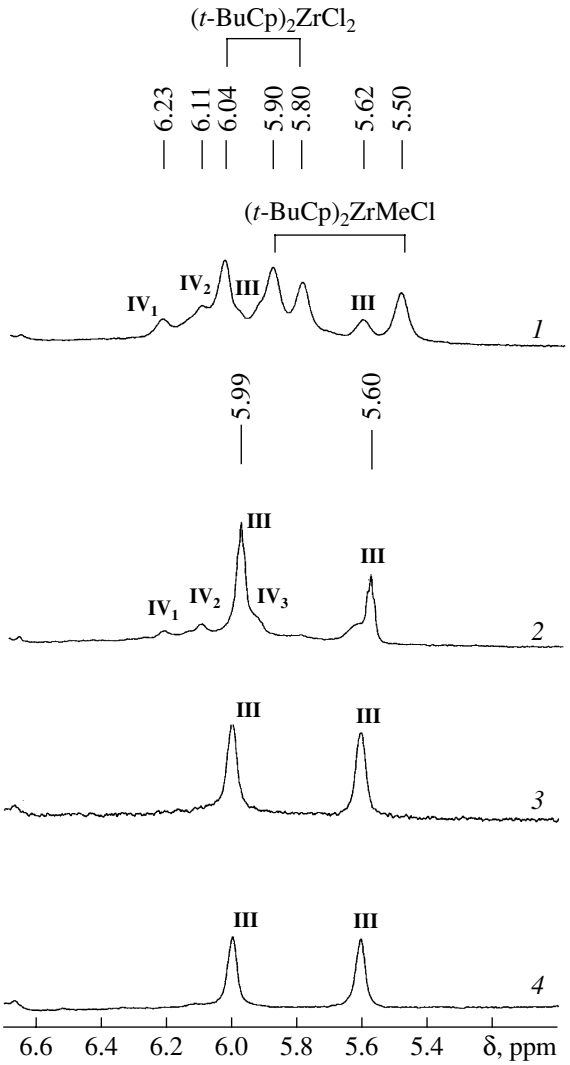

Fig. 6. ^{1}H NMR spectra of the (Cp–*t*-Bu)$_2$ZrCl$_2$/MAO system in the region of hydrogen atoms of the Cp group at Al/Zr = (*1*) 50, (*2*) 200, (*3*) 600, and (*4*) 1000; [MAO] = 0.5 mol/l, [(Cp–*t*-Bu)$_2$ZrCl$_2$] = (*1*) 10^{-2}, (*2*) 2.5×10^{-3}, (*3*) 8×10^{-4}, and (*4*) 5×10^{-4} mol/l; toluene-d$_8$, T = 20°C [9].

ratio. However, additional studies are needed to verify this assumption.

(Cp–*t*-Bu)$_2$ZrCl$_2$/MAO. At the small metal ratio of Al/Zr = 50, the initial complex (Cp–*t*-Bu)$_2$ZrCl$_2$ and the monomethylated complex (Cp–*t*-Bu)$_2$ZrClMe are mainly present in the reaction solution (Fig. 6, spectrum *1*). At Al/Zr = 200, the NMR spectrum contains an intense signal from the Zr-III complex and a series of broad signals that can be assigned to complexes of the Zr-IV type (Fig. 6, spectrum *2*). The complex Zr-III becomes a dominant species in the reaction solution as Al/Zr is further raised (Fig. 6, spectra *3* and *4*). This result distinguishes the (Cp–*t*-Bu)$_2$ZrCl$_2$/MAO catalytic system from the Cp$_2$ZrMe$_2$/MAO catalytic system. The complexes Zr-III and Zr-IV are present in the latter in comparable amounts even at Al/Zr = 1000. Probably, the bulky substituent *tert*-butyl prevents tight cation–anion contact in the (Cp–*t*-Bu)$_2$ZrCl$_2$/MAO system and the formation of a Zr-III species with the outer-sphere coordination of the anion becomes preferable. Like (Cp–*n*-Bu)$_2$ZrCl$_2$/MAO, the (Cp–*t*-Bu)$_2$ZrCl$_2$/MAO system exhibits a considerable increase in the catalytic activity as Al/Zr is increased (Table 1). Thus, the Zr-III heterodinuclear pairs can initiate ethylene polymerization and are precursors of active species in polymerization.

(Cp–R)$_2$ZrCl$_2$/MAO (R = Me, 1,2-Me$_2$, 1,2,3-Me$_3$, 1,2,4-Me$_3$, Me$_4$). The ^{1}H NMR spectrum of the (Cp–1,2,3-Me$_3$)$_2$ZrCl$_2$/MAO system (Al/Zr = 50) contains a signal of the Zr-III complex and several weaker signals, whose origin remains unclear (Fig. 7, spectrum *1*). Unlike the (Cp–R)$_2$ZrCl$_2$/MAO systems (R = *n*-Bu,

Table 1. Polymerization of ethylene in the presence of the $(Cp–R)_2ZrCl_2$/MAO (R = H, Me, *n*-Bu, *t*-Bu) catalysts

R	Al_{MAO}/Zr, mol/mol	$P_{C_2H_4}$, atm	PE yield*		Initial activity**, (kg PE) (mol Zr)$^{-1}$ (atm C_2H_4)$^{-1}$ min^{-1}
			g	(kg PE)/(mol Zr)	
H	200	2	7.7	3850	255
Me	200	5	5.2	2600	60
n-Bu	200	2	0.7	350	35
t-Bu	200	5	0.1	50	–
H	1000	2	17.1	8550	610
Me	1000	2	14.3	7150	320
n-Bu	1000	2	23.4	11700	460
t-Bu	1000	5	7.5	3750	92

* After 15 min.
** Calculated from the PE yield after 5 min.

Table 2. Polymerization of ethylene in the presence of the $(Cp–R)_2ZrCl_2$/MAO (R = H, Me, 1,2-Me_2, 1,2,3-Me_3, 1,2,4-Me_3, Me_4, Me_5) catalysts

R	Al_{MAO}/Zr, mol/mol	$P_{C_2H_4}$, atm	PE yield*		Initial activity**, (kg PE) (mol Zr)$^{-1}$ (atm C_2H_4)$^{-1}$ min^{-1}
			g	(kg PE)/(mol Zr)	
H	200	2	7.7	3850	255
Me	200	5	5.2	2600	60
1,2-Me_2	200	2	13.0	6500	470
1,2,3-Me_3	200	5	10.0	5000	102
1,2,4-Me_3	200	5	13.9	6950	134
Me_4	200	5	17.1	8550	190
Me_5	200	5	11.5	5750	145
H	1000	2	17.1	8550	610
Me	1000	2	14.3	7150	320
1,2-Me_2	1000	2	19.0	9500	520
1,2,3-Me_3	1000	5	8.6	4300	115
1,2,4-Me_3	1000	2	8.7	4350	232
Me_4	1000	2	11.6	5800	300
Me_5	1000	2	14.1	7050	445

* After 15 min.
** Calculated from the PE yield after 5 min.

t-Bu), the $(Cp–1,2,3\text{-}Me_3)_2ZrCl_2$/MAO catalytic system is dominated by the Zr-III complex already at Al/Zr = 50 (Fig. 7, spectrum *1*). Thus, several methyl substituents in the cyclopentadienyl ring make the formation of the Zr-III complexes energetically more favorable than that the formation of the Zr-IV complexes. At large Al/Zr ratios, the complex Zr-III becomes the only observable species in the solution (Fig. 7, spectra *3*, *4*). According to ^{1}H NMR data, the initial zirconium complex is quantitatively transformed into Zr-III in the $(Cp–R)_2ZrCl_2$/MAO catalytic systems (R = 1,2,3-Me_3, 1,2,4-Me_3, Me_4) already at Al/Zr = 200 [9]. Under the assumption that the catalytic activity increases with an increase in the concentration of Zr-III complexes, it should be expected that the catalytic activity in the Al/Zr = 200–1000 region will vary much more widely in the $(Cp–R)_2ZrCl_2$ (R = *n*-Bu, *t*-Bu) systems than in the $(Cp–R)_2ZrCl_2$ (R = 1,2,3-Me_3, 1,2,4-Me_3, Me_4) systems. This agrees completely with experimental data (Tables 1, 2). Thus, for most of the catalytic systems considered, the major precursors of active species of polymerization are Zr-III heterodinuclear ion pairs. This conclusion is in good agreement with the results of similar studies of the $(Cp–R)_2ZrCl_2/AlMe_3/CPh_3^+B(C_6F_5)_4^-$

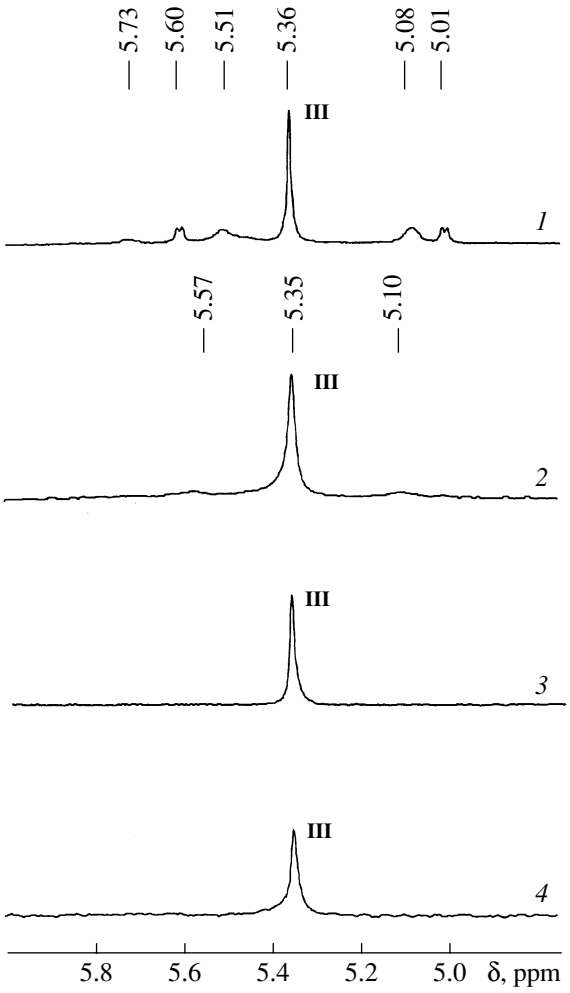

Fig. 7. ^{1}H NMR spectra of the $(Cp–1,2,3\text{-}Me_3)_2ZrCl_2$/MAO system in the region of hydrogen atoms of the Cp group at Al/Zr = (*1*) 50, (*2*) 200, (*3*) 600, and (*4*) 1000; [MAO] = 0.5 mol/l, $[(Cp–1,2,3\text{-}Me_3)_2ZrCl_2]$ = (*1*) 10^{-2}, (*2*) 2.5×10^{-3}, (*3*) 8×10^{-4}, and (*4*) 5×10^{-4} mol/l; toluene-d_8, T = 20°C [9].

catalytic systems (R = H, Me, 1,2-Me_2, 1,2,3-Me_3, 1,2,4-Me_3, Me_4, Me_5, *t*-Bu, *n*-Bu). According to ^{1}H NMR data, these systems contain only the $[(Cp–R)_2Zr(\mu\text{-}Me)_2AlMe_2]^+B(C_6F_5)_4^-$ complexes bearing the same cation as the Zr-III intermediates. The systems considered show high catalytic activities [9].

Bridged metallocene/MAO systems. A wide range of L_2ZrCl_2/MAO and L_2TiCl_2/MAO catalytic systems were studied. According to ^{1}H NMR data, for all the catalysts (rac-$C_2H_4(Ind)_2ZrCl_2$, rac-$Me_2Si(Ind)_2ZrCl_2$, rac-$Me_2Si(1\text{-}Ind\text{-}2\text{-}Me)_2ZrCl_2$, rac-$C_2H_4(1\text{-}Ind\text{-}4,5,6,7\text{-}H_4)_2ZrCl_2$, rac-$Me_2Si(2\text{-}Me\text{-}Benzind)_2ZrCl_2$, rac-$Me_2Si(1\text{-}Ind\text{-}2\text{-}Me\text{-}4\text{-}Ph)_2ZrCl_2$, $(1\text{-}Ind\text{-}2\text{-}Me)_2ZrCl_2$, $Me_2C(Cp)(Flu)ZrCl_2$, $Me_2C(Cp–3\text{-}Me)(Flu)ZrCl_2$, $Me_2Si(Flu)_2ZrCl_2$, rac-$C_2H_4(Ind)_2TiCl_2$, and rac-$Me_2Si(2\text{-}Me\text{-}Benzind)_2TiMe_2$), the complexes

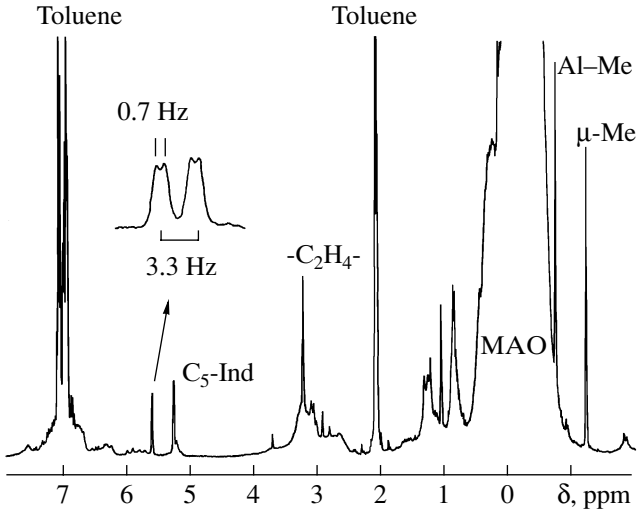

Fig. 8. ^{1}H NMR spectrum of $[rac\text{-}C_2H_4(Ind)_2Zr(\mu\text{-}Me)_2AlMe_2]^+[Me\text{-}MAO]^-$ in toluene-d_8 at 20°C; [Zr] = 3×10^{-3} mol/l, Al/Zr = 300 [9].

$[L_2Zr(\mu\text{-}Me)_2AlMe_2]^+[Me–MAO]^-$ (Zr-III) and $[L_2Ti(\mu\text{-}Me)_2AlMe_2]^+[Me–MAO]^-$ (Ti-III) dominate in the reaction solution at large ratios of Al/Zr > 200. Broad signals of complexes Zr-IV and Ti-IV are observed only at small ratios Al/Zr = 50–100 [9, 12]. It is likely that the substituents and the large size of the ligands prevent the formation of Zr-IV and Ti-IV complexes. The Zr-III and Ti-III complexes give rise to narrow NMR signals, facilitating their detection against the background of the intense and broad signal of MAO. By way of example, Fig. 8 shows the spectrum of the $[rac\text{-}C_2H_4(Ind)_2Zr(\mu\text{-}Me)_2AlMe_2]^+[Me–MAO]^-$ complex formed in the rac-$C_2H_4(Ind)_2ZrCl_2$/MAO system (Al/Zr = 300). The ^{1}H NMR spectra of the type III complexes containing $[Me\text{-}MAO]^-$ and $[B(C_6F_5)_4]^-$ as counterions are similar. This is illustrated by the ^{1}H NMR spectra of the $[rac\text{-}C_2H_4(Ind)_2Ti(\mu\text{-}Me)_2AlMe_2]^+[Me–MAO]^-$ and $[rac\text{-}C_2H_4(Ind)_2Ti(\mu\text{-}Me)_2AlMe_2]^+[B(C_6F_5)_4]^-$ complexes (Fig. 9).

The Zr-III complexes in the L_2ZrCl_2/MAO catalytic systems are stable for several weeks at room temperature, whereas the NMR signals of the Ti-III complexes in the L_2TiCl_2/MAO catalytic systems disappear in 1–2 days. To elucidate the cause of the lower stability of Ti-III, we studied the reaction of rac-$C_2H_4(Ind)_2TiCl_2$ with Al_2Me_6 ([Ti] = 0.001 mol/l, Al/Ti = 20, toluene, T = 20°C) by the ESR method. The ESR spectrum recorded 1 day after the beginning of the reaction contains a signal with g_0 = 1.978 and a hyperfine structure from Ti and Al (a_{Ti} = 12 G, a_{Al} = 2.3 G) [12]. The intensity of the signal indicates the complete reduction of Ti^{4+} to Ti^{3+}. The observed ESR spectrum, with the hyperfine structure from both Ti and Al, is due to a heterodinuclear complex with the hypothetical structure $[rac\text{-}C_2H_4(Ind)_2Ti^{III}(\mu\text{-}Me)_2AlMe_2]$. The similar com-

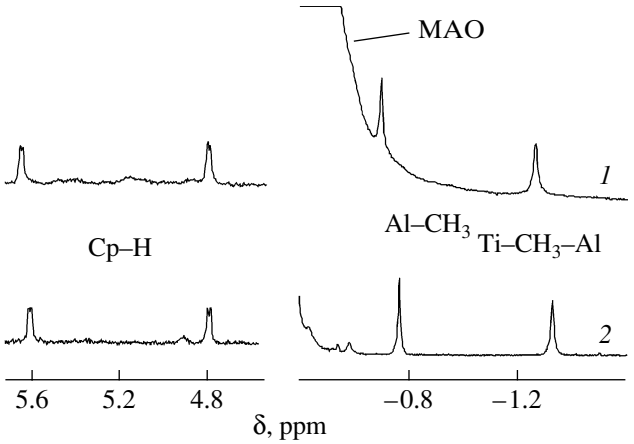

Fig. 9. ^{1}H NMR spectra of the systems (a) [rac-$C_2H_4(Ind)_2TiCl_2$ + MAO] (Al/Zr = 200) and (*2*) rac-$C_2H_4(Ind)_2TiCl_2/Al_2Me_6/CPh_3^+B(C_6F_5)_4^-$ (Al/Zr/B = 1 : 20 :1); toluene-d_8, T = 20°C [12].

plex $[Cp_2Ti^{III}(\mu\text{-}Me)_2AlMe_2]$ gives rise to an ESR signal with g_0 = 1.977 and an unresolved structure from the aluminum atom [22]. Triisobutylaluminum (TIBA) possesses much stronger reducing properties than Al_2Me_6. The addition of 10 equivalents of TIBA to a solution of rac-$C_2H_4(Ind)_2TiCl_2$ results in the immediate reduction of Ti^{4+} to Ti^{3+}. The observed ESR spectrum contains two signals. The signal with g_0 = 1.978 has a hyperfine structure from aluminum (a_{Al} = 1.8 G) and can be assigned to a complex of the rac-$C_2H_4(Ind)_2Ti^{III}(\mu\text{-}R)_2AlR_2$ type, and the other signal (g = 1.986) is a doublet (a_H = 5.5 G) and belongs to a hydrido complex of Ti^{3+} [12]. Note that, according to ESR data, the rate of Ti^{4+} reduction in the L_2TiCl_2/MAO catalytic systems is considerably higher in the presence of the monomer (ethylene or propylene). Thus, the reduction of Ti^{4+} to Ti^{3+} is the main pathway of fast activity loss by the titanocene catalysts of polymerization.

Summarizing the above results, we can conclude the following. Under conditions close to real polymerization (Al/Zr > 200), the reaction solutions of all the catalytic systems considered, namely, L_2ZrCl_2/MAO and L_2TiCl_2/MAO, contain intermediates of two types: heterodinuclear ion pairs $[L_2\mathbf{M}(\mu\text{-}Me)_2AlMe_2]^+[Me\text{–}MAO]^-$ (**III**) and zwitterionic intermediates $L_2\mathbf{M}Me^+\!\!\leftarrow\!\!-Me\text{–}Al^-\equiv MAO$ (**IV**) (**M** = Zr or Ti).

The relative concentration of complexes **III** increases with an increase in the Al/Zr ratio. Complexes **III** are characterized by narrow NMR signals, whereas broad NMR signals are characteristic of complexes **IV**. Complexes **IV** with different $[Me\text{–}MAO]^-$ counterions can exhibit different NMR signals, whereas the NMR spectra of complexes **III** are poorly sensitive to the change of the outer-sphere $[Me\text{–}MAO]^-$ counterions.

The polymerization activity of the catalytic systems increases with an increase in the proportion of intermediates **III** in the reaction solution. Thus, intermediates **III** can be precursors of active species of polymerization.

Methyl substituents in the cyclopentadienyl ring stabilize complexes **III** relative to intermediates **IV**.

The catalytic activity of the L_2TiCl_2/MAO systems decreases much more rapidly than that of the L_2ZrCl_2/MAO systems due to the fast reduction of Ti^{4+} to Ti^{3+}.

Structures of the Intermediates Resulting from the Activation of $(C_5Me_5)TiCl_3$, $[(Me_4C_5)SiMe_2N\text{-}t\text{-}Bu]TiCl_2$, $Me_4Si_2(2\text{-}Ind\text{-}4,5,6,7\text{-}H_4)ZrCl_2$, and $Me_4Si_2(2\text{-}Ind)_2ZrCl_2$ by MAO

The metallocene catalysts considered above are predominantly transformed into heterodinuclear ion pairs of type **III** upon activation by a large excess of MAO. It might be expected that the predomination of heterodinuclear ion pairs **III** at large Al-to-metal ratios is the general property of the catalytic systems in which MAO is used as the activator. However, a later study of polymerization catalysts based on half-titanocenes [10], complexes with restricted geometry [11], and complexes with disilylene bridges showed that their activation results primarily in zwitterionic complexes of type **IV**.

$(C_5Me_5)TiMe_3$/MAO. The ^{13}C NMR spectrum of the sample obtained by the addition of ^{13}C-enriched MAO to a solution of $(C_5Me_5)TiMe_3$ in toluene-d_8 contains Ti–Me signals from complexes of three types (**V**–**VII**) (Fig. 10, spectrum *1*) [10]. No signals from Ti–Me groups were observed when usual MAO was used (Fig. 10, spectrum *2*). Complex **V** is a weak $(C_5Me_5)TiMe_3$ complex with Lewis acid sites of MAO (Fig. 11). The exchange between the free $(C_5Me_5)TiMe_3$ complex and complex **V** is for the cause of the NMR signal broadening in the spectrum of complex **V**. The formation of a similar weak complex was observed between Cp_2ZrMe_2 and Lewis acid sites of MAO [8]. The very broad signal of the Ti–Me group (δ = 83 ppm, $\Delta\nu_{1/2}$ = 400 Hz), which is a superposition of several narrower signals (Fig. 10, spectrum *1*), belongs to complex **VI**. The chemical shift of this signal is close to that for the $[(C_5Me_5)TiMe_2]^+[MeB(C_6F_5)_3]^-$ complex (δ = 80–81 ppm) [23]. It is most probable that complex **VI** is the zwitterionic intermediate $(C_5Me_5)Me_2Ti^+\!\!\leftarrow\!\!-Me^-\text{–}Al\equiv MAO$ (Fig. 11). Unfortunately, we failed to observe the ^{13}C NMR signal of the Ti–Me–Al group in complex **VI** because of its large width. It seems reasonable to identify complex **VII** with a narrow Ti–Me signal as the $[(C_5Me_5)TiMe(\mu\text{-}Me)_2AlMe_2]^+[Me\text{–}MAO]^-$ complex. However, since we failed to observe $[(C_5Me_5)TiMe(\mu\text{-}$

$Me)_2AlMe_2]^+[B(C_6F_5)_4]^-$ in borate systems, additional arguments in favor of this assumption are needed.

According to NMR data, under conditions close to real polymerization (Al/Ti > 200), complex **VI** prevails in the $(C_5Me_5)TiCl_3$/MAO and $(C_5Me_5)TiMe_3$/MAO catalytic systems. This complex is considerably less stable than the similar complexes $L_2ZrMe^+ \leftarrow\!\!- Me^- - Al{\equiv}MAO$ in the zirconocene/MAO catalytic systems. The NMR signals of complex **VI** disappear within 3–5 h at room temperature, whereas the $L_2ZrMe^+ \leftarrow\!\!- Me^- - Al{\equiv}MAO$ complexes are stable for several weeks at this temperature. The most probable reason for the low stability of complex **VI**, as in the case of the titanocenes, is the reduction of Ti^{4+} to Ti^{3+}. The main distinction of the half-titanocene system $(C_5Me_5)TiMe_3$/MAO from the titanocene system Cp_2TiMe_2/MAO is that, in the latter, the $[Cp_2Ti(\mu\text{-}Me)_2AlMe_2]^+[Me\text{–}MAO]^-$ heterodinuclear ion pairs prevail at large Al/Ti ratios, whereas the $(C_5Me_5)Me_2Ti^+ \leftarrow\!\!- Me^- - Al{\equiv}MAO$ zwitterionic intermediates dominate the $(C_5Me_5)TiMe_3$/MAO system.

$[(Me_4C_5)SiMe_2N\text{-}t\text{-}Bu]TiCl_2$/MAO and $[(Me_4C_5)SiMe_2N\text{-}t\text{-}Bu]TiMe_2$/MAO. The ^{13}C NMR spectra of the samples obtained by the addition of ^{13}C-enriched MAO to solutions of $[(Me_4C_5)SiMe_2N\text{-}t\text{-}Bu]TiCl_2$ and $[(Me_4C_5)SiMe_2N\text{-}t\text{-}Bu]TiMe_2$ in toluene at 20°C (Al/Ti = 100) contained a broad, nonuniformly broadened signal of the Ti–Me group at δ = 68 ppm ($\Delta\nu_{1/2}$ = 170 Hz) [11]. This broad signal is due to the zwitterionic intermediate $[(Me_4C_5)SiMe_2N\text{-}t\text{-}Bu]TiMe^{(+)} \leftarrow\!\!- Me\text{–}Al^{(-)}{\equiv}MAO$ because the heterodinuclear ion pairs with the outer-sphere coordination of $[Me\text{–}MAO]^-$ are characterized by narrow lines in the NMR spectra. NMR signals from Ti–Me with similar shifts (61.99 and 60.5 ppm) were observed earlier [24] for two diastereomers of the $[(Me_4C_5)SiMe_2N\text{-}t\text{-}Bu]TiMe^{(+)} \leftarrow\!\!- PBA^{(-)}$ zwitterionic complex (PBA^- is tris(2,2',2"-nonafluorobiphenyl)fluoroaluminate).

Thus, in contrast to the L_2TiCl_2/MAO catalytic systems, no $[LTi(\mu\text{-}Me)_2AlMe_2]^+$ heterodinuclear species were found in the systems based on the titanium complexes of restricted geometry, and zwitterionic intermediates with the inner-sphere coordination $[Me\text{–}MAO]^-$ are mainly present in the solution. A similar situation was observed for the $(C_5Me_5)TiMe_3$/MAO catalytic system [10]. Probably, for the complexes more open than the metallocenes, the tight inner-sphere coordination of $[Me\text{–}MAO]^-$ with the formation of type **IV** species is preferential compared to the formation of type **III** species with the outer-sphere coordination of $[Me\text{–}MAO]^-$.

$Me_4Si_2(2\text{-}Ind\text{-}4,5,6,7\text{-}H_4)ZrCl_2$/MAO and $Me_4Si_2(2\text{-}Ind)_2ZrCl_2$/MAO. The complexes with the disilylene bridges $Me_4Si_2(2\text{-}Ind)_2ZrCl_2$ and $Me_4Si_2(2\text{-}Ind\text{-}4,5,6,7\text{-}H_4)_2ZrCl_2$ are more open than the metallocenes with one silylene bridge. Therefore, it might be expected that, for the activation of these complexes by MAO, the zwitterionic complexes of type **IV** would prevail in the solution even at large Al/Zr ratios. In accordance with this assumption, only very broad signals of type **IV** complexes were observed even at large Al/Zr ratios (400–1000) for the reaction of $Me_4Si_2(2\text{-}Ind\text{-}4,5,6,7\text{-}H_4)ZrCl_2$ with MAO. For the interaction of the $Me_4Si_2(2\text{-}Ind)_2ZrCl_2$ complex with MAO, both the narrow signals of complex **III** and the broad signals of the type **IV** complexes were observed at Al/Zr = 1000. Thus, complexes **III** and **IV** both can be precursors of active species of polymerization, depending on the structure of the initial complex.

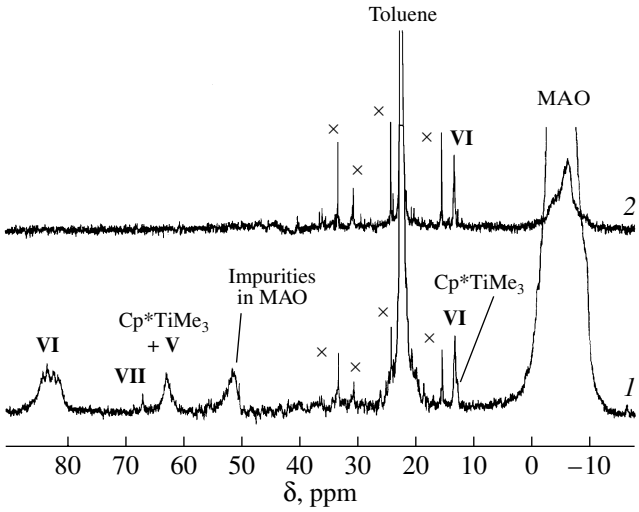

Fig. 10. ^{13}C NMR spectra of $(C_5Me_5)TiMe_3$ 1 h after the addition of MAO (*1*) enriched in the ^{13}C isotope and (*2*) without enrichment. Admixtures in toluene are designated by asterisks [10]. $[(C_5Me_5)TiMe_3] = 0.02$ mol/l, Al/Ti = 35, toluene, $T = -10$°C.

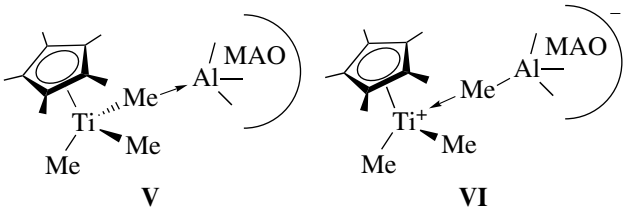

Fig. 11. Assumed structures of complexes **V** and **VI** [10].

Structures of the Intermediates Resulting from the Activation of Iron(II) Bis(imino)pyridyl Complexes by MAO and AlR_3

In the past decade, the bis(imino)pyridyl iron complexes have attracted the attention of specialists working in the area of catalytic olefin polymerization [2, 25–44]. When activated with MAO or a trialkylaluminum, these complexes efficiently catalyze the polymerization of

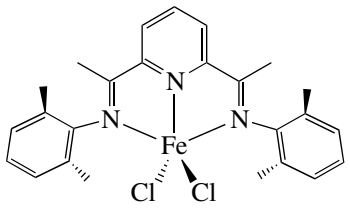

VIII

Fig. 12. Structure of complex $LFeCl_2$ (**VIII**) (L = 2,6-bis[(1-2,6-dimethylphenylimino)ethyl]pyridine).

ethylene into linear polyethylene. Several studies aimed at elucidating the mechanism of the catalytic effect of these catalysts were published [33–42]. We determined, by ^1H and ^2H NMR, the structures of the intermediates formed upon the activation of the $LFeCl_2$ complex (**VIII**) (L = 2,6-bis[(1-2,6-dimethylphenylimino)ethyl]pyridine) with such activators as MAO and trimethyl-, triisobutyl-, and trioctylaluminums [35, 37, 42]. The structure of complex **VIII** is presented in Fig. 12. In order to assign the signals in the ^1H NMR spectra of the paramagnetic iron(II) complexes, we compared the integrated intensities of the signals and their width (the latter correlates with the distance between the atom and the disturbing paramagnetic center). It was found that initial complex **VIII** interacts with MAO to be converted mainly into complex **IX** (L = Cl) at Al/Fe = 10–200 and into complex **IX** (L = Me) at Al/Fe = 500–1000 (Figs. 13, 14). Compounds **IX** and **X** are heterodinuclear iron(II) complexes in which the $AlMe_2$ group is bonded to the initial complex. This is unambiguously indicated by the ^1H NMR signal from the $AlMe_2$ fragment designated X in Fig. 14. The assignment of the signal from X to the $AlMe_2$ fragment was confirmed by ^2H NMR data. Deuterated MAO and $Al(CD_3)_3$ were used in these experiments. The ionic nature of compound **IX** (L = Cl, Me) was inferred from the similarity between the ^1H NMR spectra of **IX** (L = Cl, Me) and the complex ($[LFe^{II}(\mu\text{-}Me)_2AlMe_2]^+[B(C_6F_5)_4]^-$), observed in the **VIII** + $AlMe_3$ + $CPh_3B(C_6F_5)_4$ system. The formation of ion pairs should be expected in this system.

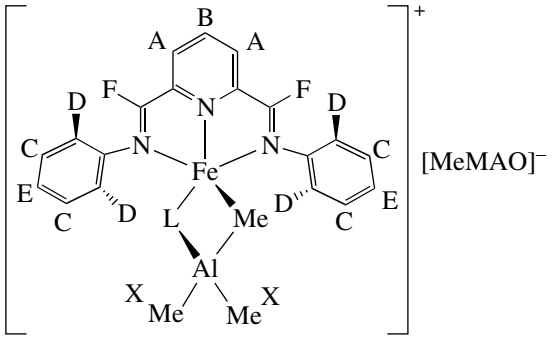

IX: L = Cl^-
L = Me^-

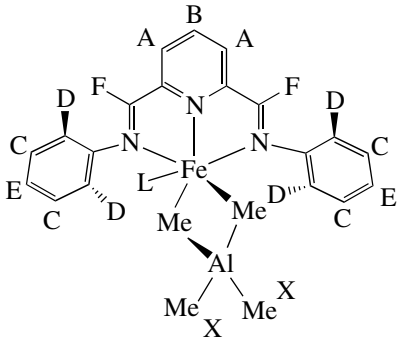

X: L = Cl^- or Me^-,

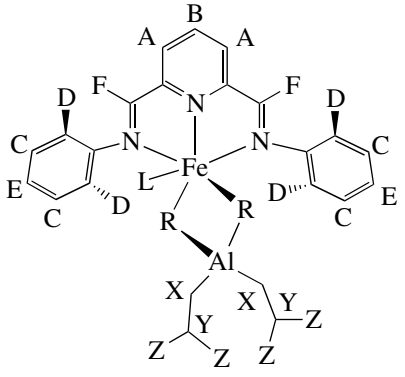

XI: L = Cl^- or R^-,
R = $CH_2CH(CH_3)_2$

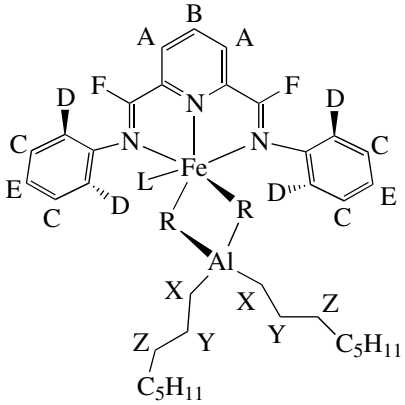

XII: L = Cl^- or R^-,
R = $CH_2C_7H_{15}$

Fig. 13. Assumed structures of complexes **IX–XII** [37].

The ^{1}H NMR spectra of the **VIII**/$AlMe_3$ system are similar to those for other **VIII**/AlR_3 systems and differ substantially from the spectra of complexes **IX** (L = Cl) and **IX** (L = Me) (Fig. 14). From this fact, we conclude that the neutral species $L(Me)Fe^{II}(\mu\text{-}Me)_2AlMe_2$ or $L(Cl)Fe^{II}(\mu\text{-}Me)_2AlMe_2$ is formed in the **VIII**/$AlMe_3$ system, whereas the ion pairs $[LFe^{II}(\mu\text{-}Me)(\mu\text{-}Cl)AlMe_2]^+[Me\text{–}MAO]^-$ and $[LFe^{II}(\mu\text{-}Me)_2AlMe_2]^+[Me\text{–}MAO]^-$ are formed in the **VIII**/MAO system. The signals of $Al(CD_3)_2$ and Fe–CD_3–Al (36 and 630 ppm, respectively) were observed in the ^{2}H NMR spectra of complex **X** [37]. Since the ^{1}H NMR spectra of the **VIII**/$AlMe_3$ and **VIII**/AlR_3 catalytic systems are similar (Fig. 14), it can be assumed that similar complexes, namely, $L(Me)Fe^{II}(\mu\text{-}R)_2AlR_2$ or $L(Cl)Fe^{II}(\mu\text{-}R)_2AlR_2$ (**XI**, **XII**), are formed in these catalytic systems (Fig. 13). According to NMR data, under conditions similar to the polymerization conditions, the **VIII**/MAO catalytic system is dominated by heterodinuclear ion pairs **IX**, like the metallocene/MAO catalytic systems.

Activity data for the **VIII** + MAO and **VIII** + AlR_3 catalytic systems are presented in Table 3. It can be seen that complex **VIII** shows similar activities with all activators. However, the molecular-weight distribution of the polymer for the **VIII** + MAO system is much narrower than that for **VIII** +AlR_3 (Table 3). Therefore, different active species lead polymerization in the **VIII** + MAO and **VIII** +AlR_3 systems, as follows from the results of NMR studies. The stability of the **VIII** +AlR_3 catalytic system is much lower than the stability of the **VIII** + MAO system. In the case of **VIII** + AlR_3, the activity decreases by a factor of 5 in the first 15 min after the beginning of polymerization, whereas it is approximately unchanged over 30 min for the **VIII** + MAO system.

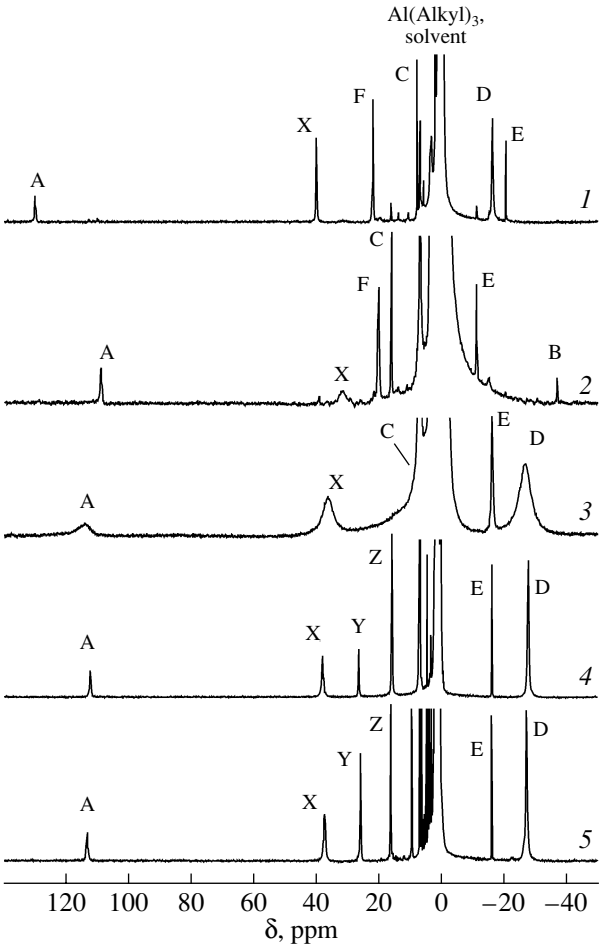

Fig. 14. ^{1}H NMR spectra of complexes **IX**–**XII** formed upon the interaction of $LFeCl_2$ (**VIII**) with different activators: (*1*) MAO, Al/Fe = 100; (*2*) MAO, Al/Fe = 1000; (*3*) Al_2Me_6, Al/Fe = 30; (*4*) Al(*i*-Bu)$_3$, Al/Fe = 30; (*5*) Al(*n*-Oct)$_3$, Al/Fe = 30. Toluene-d_8, T = 20°C.

Structures of the Intermediates Resulting from the Activation of Titanium Bis(phenoxyimine) Complexes by MAO and $AlMe_3$/$[CPh_3]^+[B(C_6F_5)_4]^-$

The zirconium and titanium bis(phenoxyimine) complexes activated by MAO and $AlMe_3/[CPh_3]^+[B(C_6F_5)_4]^-$ lead the polymerization of ethylene and other α-olefins to yield polymers with a wide range of properties interesting for practical use [45–60]. In recent years, specialists have been greatly interested in the "living" polymerization of olefins in the presence of the fluorinated bis(phenoxyimine) titanium complexes activated by MAO or the Al(*i*-Bu)$_3$/$[CPh_3]^+[B(C_6F_5)_4]^-$ system [50]. Using ^{1}H, ^{13}C, and ^{19}F NMR spectroscopy, we determined the

Table 3. Polymerization of ethylene in the presence of $LFeCl_2$ (**VIII**) activated by different organoaluminum compounds

Activator	Activity, (kg PE) (mol Fe) (atm C_2H_4) min^{-1}	$M_n \times 10^{-3}$	$M_w \times 10^{-3}$	M_w/M_n
MAO	490	13.5	45	3.3
$AlMe_3$	450	8.9	106	12
Al(*i*-Bu)$_3$	375	10.7	115	10.8
Al(*n*-Oct)$_3$	510	7.3	46	6.3

Note: Polymerization conditions: T = 35°C, toluene, reaction time of 15 min, [Fe] = 1.4×10^{-5} mol/l, Al (cocatalyst)/Fe = 500 (mol/mol), and $P_{C_2H_4}$ = 2 atm.

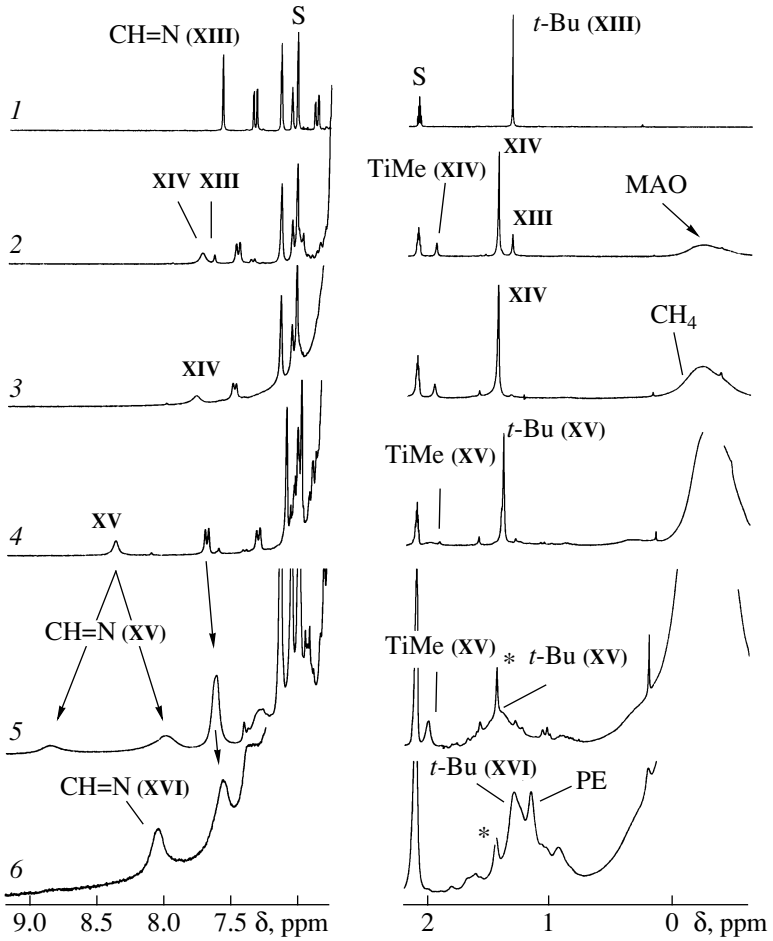

Fig. 15. ^{1}H NMR spectra of (*1*) initial complex **XIII** and (*2*–*6*) **XIII**/MAO samples: (*2*) Al/Ti = 10, 20°C; (*3*) Al/Ti = 15, 20°C; (*4*) Al/Ti = 50, 20°C; (*5*) Al/Ti = 50, –20°C; (*6*) sample *5* 15 min after the addition of 20 equivalents of ethylene at –20°C. [**XIII**] = 2.5×10^{-2} mol/l, toluene-d_8. The signals of the *t*-Bu group of the $LAlMe_2$ complex (product of catalyst deactivation) are designated by arrows (S designates the signals of the solvent).

nature of the active species initiating and continuing ethylene polymerization in the L_2TiCl_2/MAO and $L_2TiCl_2/AlMe_3/[CPh_3]^+[B(C_6F_5)_4]^-$ catalytic systems, where L_2TiCl_2 is bis[N-3-*tert*-butylsalicylidene)-2,3,4,5,6-pentafluoroanilinato]titanium(IV) dichloride (**XIII**) [14].

The ^{1}H NMR spectrum of initial complex **XIII** in a toluene-d_8–1,2-difluorobenzene (9 : 1) mixture has narrow, well-resolved signals (Fig. 15, spectrum *4*; Table 4). After MAO was added (Al/Ti = 15), the major portion of complex **XIII** was converted into the $L_2TiMeCl$ complex (**XIV**) (Fig. 15, spectra *2*, *3*; Table 4). At 20°C, the signal from the imine group of complex **XIV** is a broadened singlet (7.70 ppm). At –40°C, this signal is split into two signals (7.55 and 7.34 ppm) because of the nonequivalence of the two phenoxyimine ligands. The experiments with ^{13}C-enriched MAO showed that the signal at δ = 79.3 ppm ($\Delta\nu_{1/2}$ = 40 Hz) is due to the Ti–$^{13}\underline{C}H_3$ group of complex **XIV**.

As the Al/Ti ratio is increased in the **XIII**/MAO system, complex **XV** appears. At Al/Ti = 50, it becomes the dominant species in the reaction solution (Fig. 15, spectrum *4*; Table 4). The ^{13}C NMR signal of the Ti–Me group of complex **XV** is observed at 87.2 ppm ($\Delta\nu_{1/2}$ = 42 Hz, –20°C, toluene-d_8–1,2-difluorobenzene). The value $^1J_{CH}$ = 127 Hz, determined for the peak at δ = 87.2 ppm, is characteristic of terminal Ti–Me groups (for the bridging Ti–Me–Al groups, the $^1J_{CH}$ value would be 113–118 Hz). These data and the downfield shift of the signal from the Ti–Me group of complex **XV** (87.2 ppm) relative to the corresponding signal of $L_2TiMeCl$ (79.3 ppm) agree with the earlier assumption that **XV** is a cationic complex containing a terminal Ti–Me group [56]. The comparatively narrow NMR signals corresponding to complex **XV** indicate that its counterion $[Me–MAO]^-$ is located in the outer coordination sphere of titanium and the vacant coordination site is occupied by a solvent molecule (S). Thus, complex **XIII** reacts with MAO at large Al/Ti ratios to form the outer-sphere ion pair $[L_2TiMe(S)]^+[Me–MAO]^-$

Table 4. Chemical shifts (ppm) of ^{13}C and ^{1}H NMR signals (linewidths $\Delta\nu_{1/2}$ (Hz) and spin–spin interaction constants $^{1}J_{CH}$ (Hz)) for complexes **XIII**–**XV** in a toluene-d_8 + 1,2-difluorobenzene mixture

Complex	Al/Ti	T, °C	^{1}H (N=CH)	^{13}C (Ti–Me)	^{1}H (Ti–Me)	^{13}C (*t*-Bu)	^{1}H (*t*-Bu)
L_2TiCl_2 (**XIII**)	–	20	7.56	–	–	–	1.35
$L_2TiClMe$ (**XIV**)	15	20	7.74 ($\Delta\nu_{1/2}$ = 25)	79.3[a] ($\Delta\nu_{1/2}$ = 40)	1.97 ($\Delta\nu_{1/2}$ = 7)	29.3	1.46
$L_2TiClMe$ (**XIV**)	15	–40	7.55, 7.34	–	~2.1[b]	–	1.53, 1.46
$[L_2TiMe(S)]^+$ MeMAO$^-$ (**XV**)	50	20	8.32 ($\Delta\nu_{1/2}$ = 13)	–	2.00 ($\Delta\nu_{1/2}$ = 30)	–	1.40
$[L_2TiMe(S)]^+$ MeMAO$^-$ (**XV**)	50	–20	8.81, 7.90	87.2 ($\Delta\nu_{1/2}$ = 42)[c] (J^1_{CH} = 127)	2.0 ($\Delta\nu_{1/2}$ = 14)	29.5	1.4 ($\Delta\nu_{1/2}$ = 40)
$[L_2TiP]^+$ MeMAO$^-$ (**XVI**)	50	–20	8.10 ($\Delta\nu_{1/2}$ = 35)	–	–	–	1.29[d]
$LAlMe_2$	50	20	7.38	–	–	–	1.46

[a] At –2°C.

[b] Overlaps with the residual peak of toluene-d_8.

[c] $\Delta\nu_{1/2}$ = 270 Hz at –2°C.

[d] ^{13}C: 14.6 ppm ($H_3{}^{13}\underline{C}$–$(CH_2)_n$–Ti), 23.4 ppm (d, $^{1}J_{CC}$ = 34.8 Hz, $H_3{}^{12}C$–$H_2{}^{13}\underline{C}$–$H_2{}^{13}C$–$(CH_2)_n$–$H_2{}^{13}C$–Ti), 32.6 ppm ($H_3{}^{12}C$–$H_2{}^{13}C$–$H_2{}^{13}\underline{C}$–$(CH_2)_n$–$H_2{}^{13}C$–Ti), 111.5 ($H_3{}^{12}C$–$H_2{}^{13}C$–$H_2{}^{13}C$–$(CH_2)_n$–$H_2{}^{13}\underline{C}$–Ti), ^{1}H: 1.16 ppm ($H_3{}^{13}C$–$(\underline{CH_2})_n$–Ti).

(**XV**). Probably, the bulky phenoxyimine ligands prevent the formation of $[L_2Ti(\mu\text{-}Me)_2AlMe_2]^+[Me\text{–}MAO]^-$ heterodinuclear complexes characteristic of metallocene systems.

Ion pair **XV** is unstable at room temperature. The main causes of its decomposition are ligand transfer to aluminum, yielding an $LAlMe_2$ complex, and the reduction of Ti^{4+} to Ti^{3+}.

The **XIII**/MAO system is a "living" catalyst for ethylene and propylene polymerization. After 20 equivalents of ethylene were added to the **XIII**/^{13}C-MAO system (Al/Zr = 50), the peak of Ti–$^{13}CH_3$ (87.2 ppm) of complex **XV** disappeared and the corresponding isotopically enriched signal at 14.6 ppm of the terminal carbon atom "a" appeared (Fig. 16, Scheme 1).

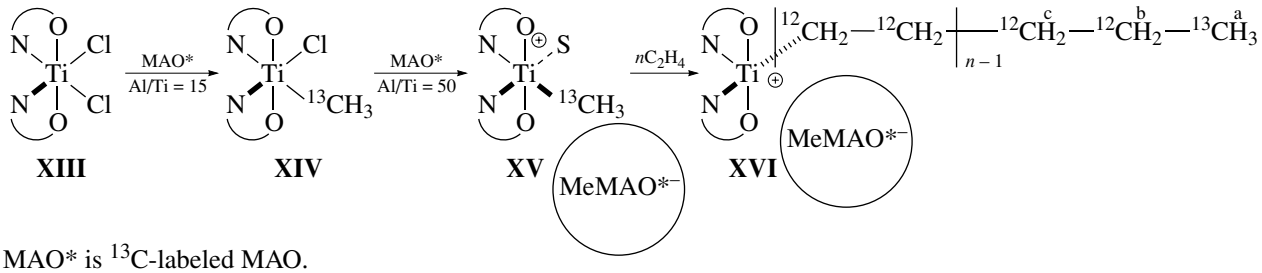

XIII **XIV** **XV** **XVI**

MAO* is ^{13}C-labeled MAO.

Scheme 1. Formation of complexes **XVI** containing the polymer chain as one of the ligands.

This result indicates unambiguously that this is precisely **XV** that initiates ethylene polymerization. This leads to the formation of the ion pair $[L_2TiP]^+[Me\text{–}MAO]^-$ (**XVI**) (P is the polymer chain). To obtain more comprehensive information about the structure of compound **XVI**, we studied the reaction of complex **XV** with ^{13}C-enriched ethylene. After $^{13}C_2H_4$was added to a solution containing complex **XV**, three new ^{13}C NMR peaks were observed. Two peaks belonged to the methylenic protons b and c of the polymer chain, and the peak at 111.5 ppm ($\Delta\nu_{1/2}$ = 70 Hz) belonged to the Ti–CH_2 group of the Ti–P fragment in complex **XVI** (Fig. 17, Scheme 2). This is the first direct observation of an active species responsible for polymer chain propagation with the titanium bis(phenoxyimine) complex/MAO catalytic system.

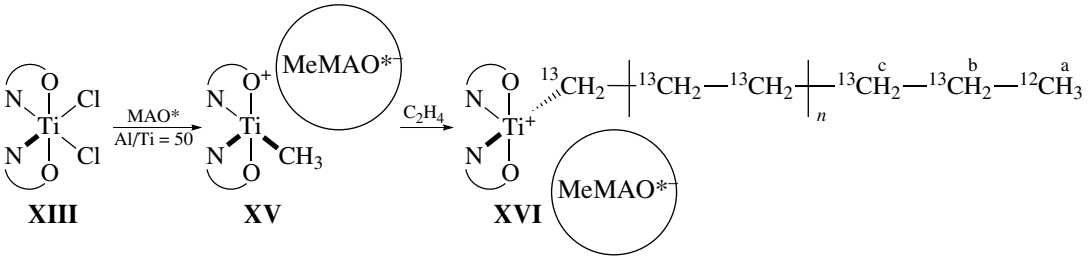

Scheme 2. Formation of complexes **XVI** containing the polymer chain labeled with ^{13}C isotope as one of the ligands.

Activation of Metallocenes with MAO Modified with Al(i-Bu)$_3$

The structures of the intermediates resulting from the reaction of MAO with different polymerization catalysts were considered above. The nature of the activator remained unchanged. In addition to the variation of the structure of the initial complexes, the modification of the activator can also be a method for affecting the catalytic activity and the structure of the polymers formed. A very large excess of MAO (Al/metal > 1000) is required for efficient activation of metallocenes and post-metallocenes. As a result, the price of MAO contributes noticeably to the cost of the resulting polymer and, hence, it is desirable to reduce the amount of activator. This can be achieved by the replacement of part of the MAO by triisobutylaluminum (TIBA). Relatively small admixtures of TIBA ($[Al]_{TIBA}/[Al]_{MAO}$ = 1 : 3) allow a smaller MAO excess to be used for the activation of metallocenes [61–64].

To elucidate the nature of the favorable effect of TIBA on the activation ability of MAO, we compared the Lewis acidities of MAO and TIBA-modified MAO [13]. The stable radical 2,2,6,6-tetramethylpiperidine-*N*-oxyl (TEMPO) was used as a probe to characterize Lewis acidity. The ESR spectrum of TEMPO coordinated with MAO differs from that of free TEMPO, which makes it possible to use TEMPO in the characterization of the acid sites of MAO. This approach is especially convenient when the ESR spectrum of coordinated TEMPO exhibits a hyperfine structure (HFS) from the aluminum atom of the acid site. Then the HFS constant (a_{Al}) serves as a measure of the Lewis acidity of the site. The larger the a_{Al} value, the higher the Lewis acidity. Using this approach, we found that MAO contains two types of Lewis acid sites (K1 and K2). For the K1 sites, $a_{Al} = 1.0 \pm 0.1$ G; for K2 sites, $a_{Al} = 1.9 \pm 0.1$ G. Therefore, the K2 sites have a higher acidity. With an increase in the number of alkyl substituents in the coordination sphere of aluminum, its Lewis acidity decreases: for the TEMPO · $AlCl_3$, a_{Al} = 9.8 G; for TEMPO · $AlCl_2Et$ a_{Al} = 6.9 G; for TEMPO · $AlClEt_2$, a_{Al} = 3.7 G. Therefore, the K1 sites can be attributed to

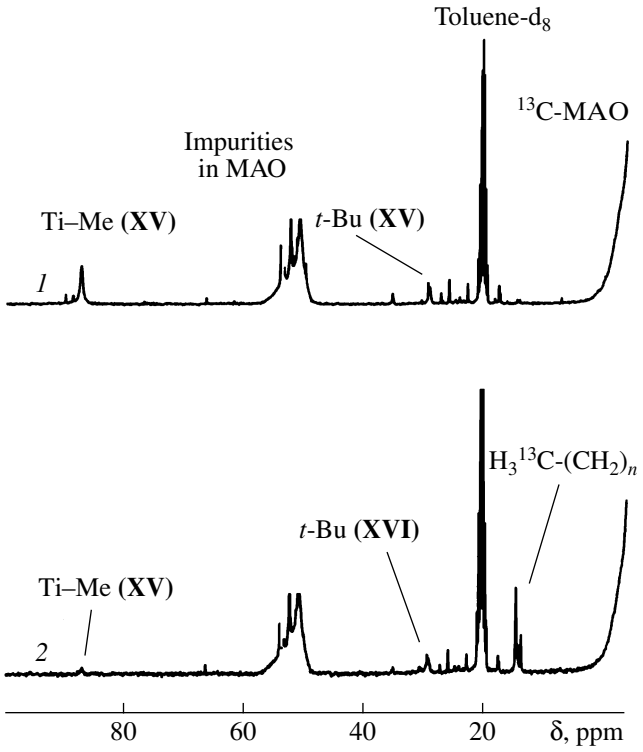

Fig. 16. ^{13}C NMR spectra of the **XIII**/^{13}C-MAO system (*1*) before and (*2*) after the addition of 20 equivalents of ethylene at –20°C. [**XIII**] = 2.5×10^{-2} mol/l, Al/Zr = 50, toluene-d_8.

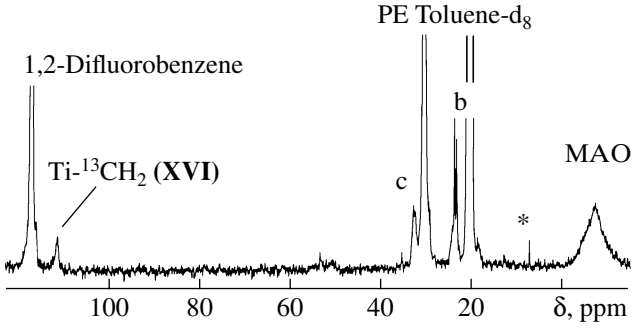

Fig. 17. ^{13}C NMR spectrum of the titanium species containing, as a ligand, the polymer chain formed in the **XIII**/MAO system after the addition of 16 equivalents of ethylene-$^{13}C_2$ at –20°C. [**XIII**] = 2.5×10^{-2} mol/l, Al/Zr = 50, toluene-d_8. Impurity $^{13}C_2H_6$ is designated by arrows. Signals b and c are the terminal methylenic protons of the polymer chain (see Scheme 2).

the coordinatively unsaturated aluminum atoms in the $AlOMe_2$ environment and the K2 sites can be assigned to the aluminum atoms in the AlO_2Me environment.

An analysis of the ESR spectra of the TEMPO + MAO + TIBA samples showed that TIBA-modified MAO also contains two types of Lewis acid sites ($K1_{TIBA}$ and $K2_{TIBA}$). For the $K1_{TIBA}$ sites, no HFS was observed on the aluminum atom, whereas for the $K2_{TIBA}$ sites $a_{Al} = 4$ G. Already small TIBA admixtures (10% with respect to MAO) result in the complete transformation of the K1 and K2 sites into the $K1_{TIBA}$ and $K2_{TIBA}$ sites. The Lewis acid sites of TIBA-modified MAO have a higher acidity than the corresponding MAO sites ($a_{Al} = 4$ G for $K2_{TIBA}$ and $a_{Al} = 1.9$ G for K2). The large $[Al]_{MAO}$/[metal] ratios required for metallocene activation are undoubtedly due to the necessity to provide a sufficient number of the strong acid sites K2. The higher acidity of the $K2_{TIBA}$ sites can explain the fact that TIBA makes it possible to use a smaller MAO excess for metallocene activation. The $K2_{TIBA}$ acid sites probably belong to aluminum atoms in the $AlO_2(i\text{-Bu})$ environment.

A comparison of the ^{1}H NMR spectra of the rac-$Me_2Si(Ind)_2ZrCl_2$/MAO and rac-$Me_2Si(Ind)_2ZrCl_2$/MMAO catalytic systems (where MMAO is the commercial sample obtained by the combined hydrolysis of $AlMe_3$ and $Al(i\text{-Bu})_3$) showed that the heterodinuclear ion pairs [rac-$Me_2Si(Ind)_2Zr(\mu\text{-}Me)_2AlMe_2]^+[MeMAO]^-$ prevailed in the solution in the first case at large ratios Al/Zr > 200, whereas [rac-$Me_2Si(Ind)_2Zr(\mu\text{-}Me)_2Al(i\text{-Bu})_2]^+$ [Me-(MAO)+TIBA)]$^-$ and [rac-$Me_2Si(Ind)_2Zr(\mu\text{-}Me)_2Al(i\text{-Bu})Me]^+$[Me–(MAO + TIBA)]$^-$ mixed ion pairs were mainly present in the solution in the second case [13, 65]. The enhancement of the activation ability of MAO upon TIBA addition can be related to both the higher strength of the Lewis acid sites $AlO_2(i\text{-Bu})$ ($a_{Al} = 4$ G) compared to AlO_2Me ($a_{Al} = 1.9$ G) and the lower coordination ability of the [Me-(MAO+TIBA)]$^-$ conterion compared to those of [MeMAO]$^-$.

ACKNOWLEDGMENTS

This work was supported by the Russian Foundation for Basic Research (project nos. 03-03-33034 and 06-03-32700), the International Science Foundation (grant no. 00841), and the Royal Society (grant no. 2004/R1-FSU).

REFERENCES

1. Bochmann, M., *J. Organomet. Chem.*, 2004, vol. 689, no. 24, p. 3982.
2. Gibson, V.C. and Spitzmesser, S.K., *Chem. Rev.*, 2003, vol. 103, no. 1, p. 283.
3. Kaminsky, W., *J. Chem. Soc., Dalton Trans.*, 1998, no. 9, p. 1413.
4. Chen, E. and Marks, T.J., *Chem. Rev.*, 2000, vol. 100, no. 4, p. 1391.
5. Brintzinger, H.-H., Fischer, D., Mulhaupt, R., Rieger, B., and Waymouth, R.M., *Angew. Chem., Int. Ed. Engl.*, 1995, vol. 34, no. 9, p. 1143.
6. Matsui, S. and Fujita, T., *Catal. Today*, 2001, vol. 66, no. 1, p. 63.
7. Tritto, I., Donetti, R., Sacchi, M.C., Locatelli, P., and Zannoni, G., *Macromolecules*, 1997, vol. 30, no. 5, p. 1247.
8. Babushkin, D.E., Semikolenova, N.V., Zakharov, V.A., and Talsi, E.P., *Macromol. Chem. Phys.*, 2000, vol. 201, no. 5, p. 558.
9. Bryliakov, K.P., Semikolenova, N.V., Yudaev, D.V., Zakharov, V.A., Brintzinger, H.-H., Ystenes, M., Rytter, E., and Talsi, E.P., *J. Organomet. Chem.*, 2003, vol. 683, no. 1, p. 92.
10. Bryliakov, K.P., Semikolenova, N.V., Zakharov, V.A., and Talsi, E.P., *J. Organomet. Chem.*, 2003, vol. 683, no. 1, p. 23.
11. Bryliakov, K.P., Talsi, E.P., and Bochmann, M., *Organometallics*, 2004, vol. 23, no. 1, p. 149.
12. Bryliakov, K.P., Babushkin, D.E., Talsi, E.P., Voskoboynikov, A.Z., Gritzo, H., Schroder, L., Damrau, H-R.H., Wieser, U., Schaper, F., and Brintzinger, H-H., *Organometallics*, 2005, vol. 24, no. 5, p. 894.
13. Bryliakov, K.P., Semikolenova, N.V., Panchenko, V.N., Zakharov, V.A., Brintzinger, H.-H., and Talsi, E.P., *Macromol. Chem. Phys.*, 2006, vol. 207, no. 3, p. 327.
14. Bryliakov, K.P., Kravtsov, E.A., Pennington, D.A., Lancaster, S.J., Bochmann, M., Brintzinger, H.-H., and Talsi, E.P., *Organometallics*, 2005, vol. 24, no. 23, p. 5660.
15. Yang, X., Stern, C.L., and Marks, T.J., *J. Am. Chem. Soc.*, 1991, vol. 113, no. 9, p. 3623.
16. Yang, X., Stern, C.L., and Marks, T.J., *J. Am. Chem. Soc.*, 1994, vol. 116, no. 22, p. 10 015.
17. Jia, L., Yang, X., Stern, C.L., and Marks, T.J., *Organometallics*, 1997, vol. 16, no. 5, p. 842.
18. Chen, Y.-X., Metz, M.V., Li, L., Stern, C.L., and Marks, T.J., *J. Am. Chem. Soc.*, 1998, vol. 120, no. 25, p. 6287.
19. Bochmann, M. and Lancaster, S.J., *Angew. Chem., Int. Ed. Engl.*, 1994, vol. 33, no. 12, p. 1634.
20. Zhou, J., Lancaster, S.J., Walker, D.A., Beck, S., Thornton-Pett, M., and Bochmann, M., *J. Am. Chem. Soc.*, 2001, vol. 123, no. 2, p. 223.
21. Bochmann, M. and Sarsfield, M.J., *Organometallics*, 1998, vol. 17, no. 26, p. 5908.
22. Holton, J., Lappert, M.F., Ballard, D.G.H., Pearce, R., Atwood, J.L., and Hunter, W.E., *J. Chem. Soc., Dalton Trans.*, 1979, no. 1, p. 45.
23. Ewart, S.W., Sarsfield, M.J., Williams, E.F., and Baird, M.C., *J. Organomet. Chem.*, 1999, vol. 579, nos. 1–2, p. 106.
24. Chen, Y., Stern, C.L., and Marks, T.J., *J. Am. Chem. Soc.*, 1997, vol. 119, no. 10, p. 2582.
25. Small, B.L., Brookhart, M., and Bennett, A.M.A., *J. Am. Chem. Soc.*, 1998, vol. 120, no. 16, p. 4049.
26. Britovsek, G.J.P., Gibson, V.C., Kimberley, B.S., Maddox, P.J., McTavish, S.J., Solan, G.A., White, A.J.P., and Williams, D.J., *Chem. Commun.*, 1998, no. 7, p. 849.
27. Britovsek, G.J.P., Bruce, M., Gibson, V.C., Kimberley, B.S., Maddox, P.J., Mastroianni, S., McTavish, S.J., Red-

shaw, C., Solan, G.A., Stromberg, S., White, A.J.P., and Williams, D.J., *J. Am. Chem. Soc.*, 1999, vol. 121, no. 38, p. 8728.

28. Britovsek, G.J.P., Gibson, V.C., and Wass, D.F., *Angew. Chem., Int. Ed. Engl.*, 1999, vol. 38, no. 4, p. 428.
29. Ittel, S.D., Johnson, L.K., and Brookhart, M., *Chem. Rev.*, 2000, vol. 100, no. 4, p. 1169.
30. Mecking, S., *Angew. Chem., Int. Ed. Engl.*, 2001, vol. 40, no. 3, p. 534.
31. Babik, S.T. and Fink, G., *J. Mol. Catal.*, 2002, vol. 188, nos. 1–2, p. 245.
32. Griffiths, E.A.H., Britovsek, G.J.P., Gibson, V.C., and Gould, I.R., *Chem. Commun.*, 1999, no. 14.
33. Deng, L.Q., Margl, P., and Ziegler, T., *J. Am. Chem. Soc.*, 1999, vol. 121, no. 27, p. 6479.
34. Khoroshun, D.V., Musaev, D.G., Vreven, T., and Morokuma, K., *Organometallics*, 2001, vol. 20, no. 10, p. 2007.
35. Talsi, E.P., Babushkin, D.E., Semikolenova, N.V., Zudin, V.N., Panchenko, V.N., and Zakharov, V.A., *Macromol. Chem. Phys.*, 2001, vol. 202, no. 10, p. 2046.
36. Britovsek, G.J.P., Clentsmith, G.K.B., Gibson, V.C., Goodgame, D.M.L., McTavish, S.J., and Pankhurst, Q.A., *Catal. Commun.*, 2002, vol. 3, no. 2, p. 207.
37. Bryliakov, K.P., Semikolenova, N.V., Zakharov, V.A., and Talsi, E.P., *Organometallics*, 2004, vol. 23, no. 22, p. 5375.
38. Castro, P.M., Lahtinen, P., Axenov, K., Viidanoja, J., Kotiaho, T., Leskela, M., and Repo, T., *Organometallics*, 2005, vol. 24, no. 15, p. 3664.
39. Scott, J., Gambarotta, S., Korobkov, I., and Budzelaar, P.H.M., *J. Am. Chem. Soc.*, 2005, vol. 127, no. 37, p. 13019.
40. Scott, J., Gambarotta, S., Korobkov, I., and Budzelaar, P.H.M., *Organometalics*, 2005, vol. 24, no. 26, p. 6298.
41. Wang, S.B., Liu, D.B., Huang, R.B., Zhang, Y.D., and Mao, B.Q., *J. Mol. Catal. A: Chem.*, 2006, vol. 245, nos. 1–2, p. 122.
42. Zakharov, V.A., Semikolenova, N.V., Mikenas, T.B., Barabanov, A.A., Bukatov, G.D., Echevskaya, L.G., and Mats'ko, M.A., *Kinet. Katal.*, 2006, vol. 47, no. 2, p. 303 [*Kinet. Catal.* (Engl. Transl.), vol. 47, no. 2, p. 303].
43. Bart, S.C., Hawrelak, E.J., Lobkovky, E., and Chirik, P.J., *Organometallics*, 2005, vol. 24, no. 23, p. 5518.
44. Ivanchev, S.S., Oleinik, I.I., Ivancheva, N.I., and Oleinik, I.V., *Dokl. Phys. Chem.*, 2005, vol. 404, no. 2, p. 182.
45. Matsui, S., Mitani, M., Saito, J., Tohi, Y., Makio, H., Tanaka, H., and Fujita, T., *Chem. Lett.*, 1999, p. 1263.
46. Matsui, S., Mitani, M., Saito, J., Tohi, Y., Makio, H., Matsukawa, N., Takagi, Y., Tsuru, K., Nitabaru, M., Nakano, T., Tanaka, H., Kashiwa, N., and Fujita, T., *J. Am. Chem. Soc.*, 2001, vol. 123, no. 28, p. 6847.
47. Matsui, S. and Fujita, T., *Catal. Today*, 2001, vol. 66, no. 1, p. 63.
48. Saito, J., Mitani, M., Mohri, J., Yoshida, Y., Matsui, S., Ishii, S., Kojoh, S., Kashiwa, N., and Fujita, T., *Angew. Chem., Int. Ed. Engl.*, 2001, vol. 40, no. 15, p. 2918.
49. Mitani, M., Mohri, J., Yoshida, Y., Saito, J., Ishii, S., Tsuru, K., Matsui, S., Furuyama, R., Nakano, T., Tanaka, H., Kojoh, S., Matsugi, T., Kashiwa, N., and Fujita, T., *J. Am. Chem. Soc.*, 2002, vol. 124, no. 13, p. 3327.
50. Mitani, M., Nakano, T., and Fujita, T., *Chem. Eur. J.*, 2003, vol. 9, no. 11, p. 2396.
51. Tshuva, E.Y., Goldberg, I., and Kol, M., *J. Am. Chem. Soc.*, 2000, vol. 122, no. 43, p. 10 706.
52. Tian, J. and Coates, G.W., *Angew. Chem., Int. Ed. Engl.*, 2000, vol. 39, no. 20, p. 3626.
53. Tian, J., Hustad, P.D., and Coates, G.W., *J. Am. Chem. Soc.*, 2001, vol. 123, no. 21, p. 5134.
54. Pennington, D.A., Clegg, W., Coles, S.J., Harrington, R.W., Hursthouse, M.B., Hughes, D.L., Light, M.E., Schormann, M., Bochmann, M., and Lancaster, S.J., *J. Chem. Soc., Dalton Trans.*, 2005, no. 3, p. 561.
55. Corradini, P., Guerra, G., and Cavallo, L., *Acc. Chem. Res.*, 2004, vol. 37, no. 4, p. 231.
56. Makio, H. and Fujita, T., *Macromol. Symp.*, 2004, vol. 213, no. 1, p. 221.
57. Saito, J., Tohi, Y., Matsukawa, N., Mitani, M., and Fujita, T., *Macromolecules*, 2005, vol. 38, no. 12, p. 4955.
58. Furuyama, R., Mitani, M., Mohri, J., Mori, R., Tanaka, H., and Fujita, T., *Macromolecules*, 2005, vol. 38, no. 5, p. 1546.
59. Saito, J., Suzuki, Y., Makio, H., Tanaka, H., Onda, M., and Fujita, T., *Macromolecules*, 2006, vol. 39, p. 4023.
60. Ivanchev, S.S., Trunov, V.A., Rybakov, V.B., Al'bov, D.V., and Rogozin, D.G., *Dokl. Phys. Chem.*, 2005, vol. 404, no. 1, p. 165.
61. Kleinschmidt, R., van der Leek, Y., Reffke, M., and Fink, G., *J. Mol. Catal. A: Chem.*, 1999, vol. 148, nos. 1-2, p. 29.
62. Bhriain, N.Ni., Brintzinger, H.-H., Ruchatz, D., and Fink, G., *Macromolecules*, 2005, vol. 38, no. 6, p. 2056.
63. Shiono, T., Yoshida, S., Hagihara, H., and Ikeda, T., *Appl. Catal., A*, 2000, vol. 200, no. 1, p. 145.
64. Ioku, A., Hasan, T., Shiono, T., and Ikeda, T., *Macromol. Chem. Phys.*, 2002, vol. 203, no. 4, p. 748.
65. Babushkin, D.E. and Brintzinger, H.-H., *Chem. Eur. J.*, 2007, vol. 13 (in press).